DE-Vol. 47, Flexible Mechanisms, Dynamics, and Analysis
ASME 1992

STATIC ANALYSIS OF SPHERICAL nR KINEMATIC CHAINS WITH JOINT FRICTION

Pierre Larochelle and J. M. McCarthy
Department of Mechanical Engineering
University of California, Irvine
Irvine, California

Abstract

This paper presents the static analysis of general spherical nR simple open or closed kinematic chains with joint friction. The internal loading on each link is found to consist of a bending moment and a torsional moment. The goal of this analysis is to determine these moments which are then used in designing the link.

The moment and force balance equations for each link yields a linear system of equations which define the internal moments of the mechanism and the output torque on the driven crank for a given input torque. A Coulomb model of joint friction is used to determine the friction torque along the axis of a joint. The joint friction model requires an iterative solution.

The purpose of this algorithm is to provide a means of computing the complete internal and external loading on the members of spherical chains while including frictional effects in order to facilitate the design of a functional spherical mechanisms.

1 Introduction

Algorithms for designing spherical mechanisms to perform desired coupler motions, or to generate specific functions relating input and output angles are described by Duffy, 1980, and Chiang, 1988, and others. Our experience with the design and construction of spherical mechanisms shows that joints often jam due to link deformation under internal loading. It is apparent that designing links which can support these internal forces is central to synthesizing functional spherical mechanisms. This paper describes an analysis tool that performs a complete static loading analysis of a spherical mechanism which can be included in the standard kinematic design procedures.

We approach this problem from the point of view of robotics and formulate the Jacobian of the equivalent open chain which determines the relationships between external forces and moments and the applied joint torques. Unlike this case, we are also interested in the constraining forces and moments at each joint. We show that these moment terms can be determined from a construction similar to the Jacobian, which we define as the *link moment matrix*. The algorithm uses the link moment matrix to generate the moment balance equations for each member of the spherical chain. The moment and force balance equations for each link are the static equilibrium equations for the system. These equations take the form; $[A]\mathbf{x} = \mathbf{b}$, where $\mathbf{x}$ is the vector of unknown internal and external loads on the system. Frictional effects in the joints are modeled as a friction torque about the joint axis proportional to the remaining components of the joint moment. An iterative solution of the equilibrium equations yields the desired forces and moments. We demonstrate the algorithm by analyzing a $4R$ spherical closed chain.

2 Equilibrium Equations

In this section we formulate the static equations of equilibrium for a rigid link i connecting two revolute joints. First, the general spatial force and moment balance equations are derived. Then, we present the constraint equations associated with the requirement of spherical chains that the joint axes intersect at a point.

In our formulation all of the link forces are measured in the fixed reference frame, see Fig. 1. Therefore, the force balance equation for link i is simply,

$$-{}^0\mathbf{f}_i + {}^0\mathbf{f}_{i+1} = 0 \tag{1}$$

The superscript 0 indicates that the vector is measured in the fixed frame and the subscript i denotes that the force is applied by the $(i-1)^{th}$ link to the i^{th} link.

Now, the equation of moment balance for a general revolute spherical link i is derived. This derivation is based upon writing the moment balance equation in the form of the robotics technique of determining joint torques for a manipulator given a desired end-effector applied force and moment.

Let θ be the vector of joint angles for an nR link manipulator with τ as the vector of actuator torques, ${}^0\mathbf{f}_E$ as the force applied by the end-effector, and ${}^0\mathbf{n}_E$ as the moment applied by the end-effector. The superscipt 0 indicates that the vector is measured in the fixed frame and the subscript E denotes that the force or moment is appled by the end-effector. Then, the joint torque is related to the applied force and moment by the Jacobian, $[J(\theta)]$, of the manipulator, see Yoshikawa, 1990.

$$\tau = [J(\theta)]^T \begin{Bmatrix} {}^0\mathbf{f}_E \\ {}^0\mathbf{n}_E \end{Bmatrix} \tag{2}$$

where,

$$[J(\theta)] = [\mathbf{S}_1, \mathbf{S}_2, ..., \mathbf{S}_n]$$

and,

$$\mathbf{S}_i(\theta) = \begin{Bmatrix} {}^0\mathbf{z}_i \times {}^0\mathbf{p}_{E,i} \\ {}^0\mathbf{z}_i \end{Bmatrix} \tag{3}$$

Note that $\mathbf{S}_i(\theta)$ is related to the Plücker coordinates of the i^{th} joint axis of the manipulator. Here, ${}^0\mathbf{z}_i$ is the unit vector along

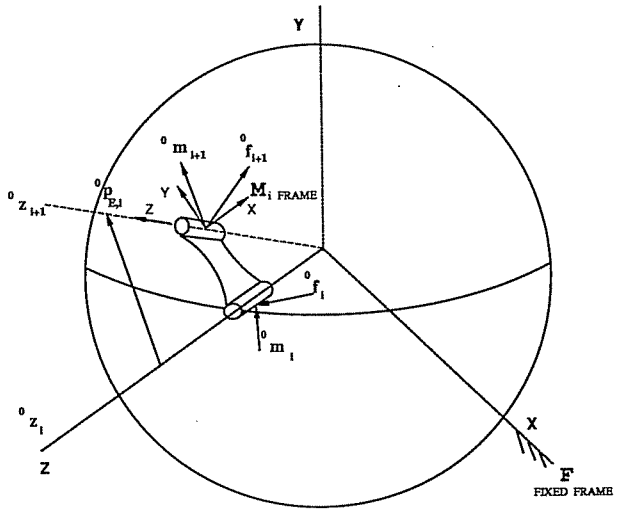

Figure 1: Free Body Diagram for a General Revolute Link

the i^{th} joint axis, and ${}^0\mathbf{p}_{E,i}$ is the vector from a point on the ${}^0\mathbf{z}_i$ axis to the end-effector.

In considering a single link of the mechanism, Eq. 2 becomes the moment balance equation for the link about its joint axis. The Jacobian, $\mathbf{S}_i(\theta)$, for this $1R$ manipulator, see Eq. 3, then relates the loads applied at the $(i+1)^{th}$ joint axis to the moment about the i^{th} joint axis.

$$\Sigma M_{o_{\mathbf{z}_i}} = 0 = -\tau_i + \mathbf{S}_i(\theta)^T \begin{Bmatrix} {}^0\mathbf{f}_E \\ {}^0\mathbf{n}_E \end{Bmatrix} \tag{4}$$

In a kinematic chain ${}^0\mathbf{f}_E$ and ${}^0\mathbf{n}_E$ are the forces that link i apply to link $i+1$. Since the links are in static equilibrium the forces and moments link i applies to link $i+1$ are reacted back to link i. Let ${}^0\mathbf{f}_{i+1}$ be the force link i applies to link $i+1$, and ${}^0\mathbf{m}_{i+1}$ be the moment link i applies to link $i+1$. Then, for link i, ${}^0\mathbf{f}_{i+1} = {}^0\mathbf{f}_E$ and ${}^0\mathbf{m}_{i+1} = {}^0\mathbf{n}_E$. Using this notation the free body diagram for a general link i is drawn, see Fig. 1. The equation of moment balance about the i^{th} joint axis is;

$$\Sigma M_{o_{\mathbf{z}_i}} = 0 = -{}^0\mathbf{m}_i \cdot {}^0\mathbf{z}_i + {}^0\mathbf{p}_{E,i} \times -{}^0\mathbf{f}_{i+1} \cdot {}^0\mathbf{z}_i - {}^0\mathbf{m}_{i+1} \cdot {}^0\mathbf{z}_i \tag{5}$$

To a complete the static analysis of a spherical link we require similar moment balance equations about each of the two axis orthogonal to the joint axis. Let ${}^0\mathbf{x}_i$, ${}^0\mathbf{y}_i$, and ${}^0\mathbf{z}_i$ be unit vectors along the (x, y, z) axis of the $(i-1)^{th}$ link reference frame. Let $\mathbf{m}_i$ be the moment link $i-1$ applies to link i, measured in the $(i-1)^{th}$ link reference frame. That is to say, $m_{ix} = {}^0\mathbf{m}_i \cdot {}^0\mathbf{x}_i$, $m_{iy} = {}^0\mathbf{m}_i \cdot {}^0\mathbf{y}_i$, and $m_{iz} = {}^0\mathbf{m}_i \cdot {}^0\mathbf{z}_i$. Then, we have from Fig. 1 and Eq. 5 that,

$$\Sigma M_{o_{\mathbf{x}_i}} = 0 = -{}^0\mathbf{m}_i \cdot {}^0\mathbf{x}_i + {}^0\mathbf{p}_{E,i} \times -{}^0\mathbf{f}_{i+1} \cdot {}^0\mathbf{x}_i - {}^0\mathbf{m}_{i+1} \cdot {}^0\mathbf{x}_i \tag{6}$$

$$\Sigma M_{o_{\mathbf{y}_i}} = 0 = -{}^0\mathbf{m}_i \cdot {}^0\mathbf{y}_i + {}^0\mathbf{p}_{E,i} \times -{}^0\mathbf{f}_{i+1} \cdot {}^0\mathbf{y}_i - {}^0\mathbf{m}_{i+1} \cdot {}^0\mathbf{y}_i \tag{7}$$

These equations written in matrix form yields,

$$m_{ix} = \begin{Bmatrix} {}^0\mathbf{x}_i \times {}^0\mathbf{p}_{E,i} \\ {}^0\mathbf{x}_i \end{Bmatrix}^T \begin{Bmatrix} {}^0\mathbf{f}_{i+1} \\ {}^0\mathbf{m}_{i+1} \end{Bmatrix} \tag{8}$$

$$m_{iy} = \begin{Bmatrix} {}^0\mathbf{y}_i \times {}^0\mathbf{p}_{E,i} \\ {}^0\mathbf{y}_i \end{Bmatrix}^T \begin{Bmatrix} {}^0\mathbf{f}_{i+1} \\ {}^0\mathbf{m}_{i+1} \end{Bmatrix} \tag{9}$$

$$m_{iz} = \begin{Bmatrix} {}^0\mathbf{z}_i \times {}^0\mathbf{p}_{E,i} \\ {}^0\mathbf{z}_i \end{Bmatrix}^T \begin{Bmatrix} {}^0\mathbf{f}_{i+1} \\ {}^0\mathbf{m}_{i+1} \end{Bmatrix} \tag{10}$$

We simplify these equations by forming the 3×3 skew-symmetric matrix $[P_i]$ corresponding to the vector ${}^0\mathbf{p}_{E,i}$. This allows ${}^0\mathbf{p}_{E,i} \times {}^0\mathbf{z}_i$ to be written as $[P_i]{}^0\mathbf{z}_i$, see McCarthy, 1990. Using this, Eq. 8, Eq. 9, and Eq. 10 are rewritten in matrix form as follows,

$$\mathbf{m}_i = [{}^0T_i]^T[P_i]{}^0\mathbf{f}_{i+1} + [{}^0T_i]^T{}^0\mathbf{m}_{i+1} \tag{11}$$

where $[{}^0T_i]$ is the 3×3 orthogonal rotation matrix which describes the orientation of the i^{th} link reference frame to the fixed frame.

In order to simplify the solving of the moment balance equations it is convenient to reformulate Eq. 11 so that all of the moment vectors are measured in their respective link reference frames. To do this let $[T_i]$ be the matrix transformation from the $(i-1)^{th}$ link reference frame to the $(i)^{th}$ link reference frame. Then,

$$[{}^0T_i] = \prod_{n=1}^{i} [T_i] \tag{12}$$

These matrices, $[T_i]$, can be used to change the reference frame of the moment vectors as follows,

$${}^0\mathbf{m}_{i+1} = [{}^0T_{i+1}]\mathbf{m}_{i+1} = [T_1][T_2]...[T_{i+1}]\mathbf{m}_{i+1} \tag{13}$$

Using Eq. 13, Eq. 11 can be written in terms of moments measured in their respective link frames in the form of Eq. 2.

$$\mathbf{m}_i = [M_{LS}]^T \begin{Bmatrix} {}^0\mathbf{f}_{i+1} \\ \mathbf{m}_{i+1} \end{Bmatrix} \tag{14}$$

where,

$$[M_{LS}] = \begin{bmatrix} [P_i]^T\,[{}^0T_i] \\ [T_{i+1}]^T \end{bmatrix} \tag{15}$$

Eq. 14 is the three moment balance equations for a general link. $[M_{LS}]$, given by Eq. 15, which we call the link moment matrix, is a 6×3 matrix derived from the geometry of the link.

Now, we present the constraint equations satisfied by the links of a spherical kinematic chain. For a spherical link i the constraint equations are as follows, see Bagci, 1971. Due to the geometry of the joints no force is transmitted from link $i-1$ to link i along the $i^{\underline{th}}$ joint axis, Eq. 16.

$$ {}^0\mathbf{f}_i \cdot {}^0\mathbf{z}_i = 0 \tag{16} $$

Furthermore, if there is no externally applied torque on the $i^{\underline{th}}$ joint axis,

$$ \mathbf{m}_i \cdot {}^0\mathbf{z}_1 = 0 \tag{17} $$

Since a revolute joint cannot support any moments.

3 Assembling the System of Equations

In this section we assemble the equilibrium equations for each link of a spherical mechanism into a system of linear equations.

Eq. 14 and Eq. 1 are the 6 equations of static equilibrium for a spherical link. These six equations written for each link of a spherical mechanism, coupled with the constraint equations, Eq. 16 and Eq. 17, form the system of linear equations to be solved. These equations are written in the form $[A]\mathbf{x} = \mathbf{b}$, where; $\mathbf{x}$ is the vector of unknown forces and moments, and $[A]$ and $\mathbf{b}$ are coefficients determined from the linear equations of static equilibrium. This system of linear equations can be solved for $\mathbf{x}$ using numerous numerical algorithms such Gauss-Seidel elimination, etc.

4 Friction

Friction is incorporated into the model as follows. The approach used here is based on Keler, 1973. First, for a given driving crank angle each of the remaining joint angles must be known. Then, for a given system configuration solve the equilibrium equations to obtain an initial solution without friction. Compute the friction at a joint axis i as follows,

$$ m_{izf} = -\mu \mathbf{MAG}(\mathbf{m}_i)\mathbf{SIGN}(\theta_{i'} - \theta_i) \tag{18} $$

where; μ is a coefficient of friction, $\mathbf{MAG}(\mathbf{m}_i)$ is the magnitude of the vector $\mathbf{m}_i$, and $\theta_{i'}$ and θ_i are the values of the joint angle one crank motion ahead of its current value, and its current value; respectively. This friction moment, m_{izf}, is introduced to the linear system of equilibrium equations by forming the vector $\mathbf{ft}$; which contains all of the friction moments. This new system of linear equations, $[A]\mathbf{x} = \mathbf{b} + \mathbf{ft}$ is then solved for $\mathbf{x}$. From this solution a new $\mathbf{ft}$ is formed. This new system is then solved. This process is repeated until we have converged upon a final solution, $\mathbf{x}$. Keler, 1973, shows that convergence will occur unless the mechanism self-locks.

5 Spherical Geometry

Recall from the above discussion that ${}^0\mathbf{z}_i$ is the unit vector along the $i^{\underline{th}}$ joint axis and that $[T_i]$ is the 3×3 orthogonal rotation matrix which describes the transformation of coordinates from the $(i-1)^{\underline{th}}$ link reference frame to the $(i)^{\underline{th}}$ link reference frame. Using the coordinates for a spherical link as defined in Denavit and Hartenberg, 1955, we have,

$$ [T_i] = \begin{bmatrix} \cos\theta_i & -\cos\alpha_i \sin\theta_i & -\sin\theta_i \sin\alpha_i \\ \sin\theta_i & \cos\alpha_i \cos\theta_i & -\cos\theta_i \sin\alpha_i \\ 0 & \sin\alpha_i & \cos\alpha_i \end{bmatrix} \tag{19} $$

where; θ_i is the rotation of link i about its axis of rotation ${}^0\mathbf{z}_i$, and α_i is the length of link i. Note that the fixed reference frame is chosen to coincide with the first joints reference frame. Therefore, $[T_1] = [I]$ and ${}^0\mathbf{z}_1 = (0,0,1)^T$. Using $[{}^0T_i]$, as defined in Eq. 12, the vectors describing the geometry of a spherical link are computed as follows,

$$ {}^0\mathbf{z}_i = [{}^0T_i]{}^0\mathbf{z}_1 \tag{20} $$

$$ {}^0\mathbf{p}_{E,i} = R({}^0\mathbf{z}_{i+1} - {}^0\mathbf{z}_i) \tag{21} $$

where R is the radius of the sphere. Using the above equations, $[M_{LS}]$ can easily be written for any link on a spherical chain.

6 Case Study: Spherical $4R$ Closed Chain

In this section we apply the static analysis methodology described above to a $4R$ spherical closed chain. Closed chains are analyzed as open chains where the fixed link of the closed chain is made to be the ground link. Therefore, a $4R$ closed chain is analyzed as a $3R$ open chain. The mechanism is shown, with the appropriate labels, in Fig. 2.

A complete static analysis of the mechanism is desired. On the driven crank a known torque is applied. In these examples, $m_{1z} = 10.0$. The mechanism chosen has the following link lengths; $\alpha_1 = 25$ deg, $\alpha_2 = 70$ deg, $\alpha_3 = 45$ deg, and $\alpha_4 = 80$ deg. Using link 1 as the driven crank results in a crank-rocker mechanism. The corresponding torque on the driven crank, as well as all of the internal forces and moments on the system, are to be solved for. Using the notation described above, the solution vector $\mathbf{x}$ has 23 components and is formed as;

$$ \mathbf{x} = ({}^0\mathbf{f}_1^T, {}^0\mathbf{f}_2^T, {}^0\mathbf{f}_3^T, {}^0\mathbf{f}_4^T, m_{1x}, m_{1y}, \mathbf{m}_2^T, \mathbf{m}_3^T, \mathbf{m}_4^T)^T \tag{22} $$

Note that m_{4z} is the desired torque on the driven crank. The 6 equations of static equilibrium are written for each of the three links using Eq. 14 and Eq. 1. This yields 18 equilibrium equations. Recall that we wish to solve for 23 unknowns. Therefore, 5 constraint equations are added to the system. Eq. 16 is written three times to constrain the internal forces that links 1,2 and 3 apply. Eq. 17, is written twice to constrain the internal moments at the two free joints of the system; the two joints on the coupler. The result is a system of 23 linear equations in 23 unknowns. The analysis was implemented using the *MATLAB* analysis package on a *DEC* 5000/200.

The driven crank angle as a function of driving crank angle is plotted in Fig. 3. Note that the driven crank velocity changes sign at a driving crank angle of 140 degrees. This is a singular configuration for the mechanism. The driven torque peaks at $\theta_1 = 140$ (degrees); though for brevity the driven torque for all crank angles is not shown here. Therefore, our load analysis will be done for driving crank angles of $0 \leq \theta_1 \leq 140$ (degrees). The driven torque is plotted in Fig. 4. The internal moments applied to the coupler are, $-m_{3x}$, which is the bending moment, and $-m_{3y}$, which we call the torsional moment. Recall that these moments are measured in the coupler's reference frame, see Fig. 1. The bending and torsional moments are plotted in Fig. 5. Note that m_{3x} has a minimum value that is 2.3 times the driving torque to the system and has a maximum that is 22.9 times the applied torque. In addition, m_{3y} is zero.

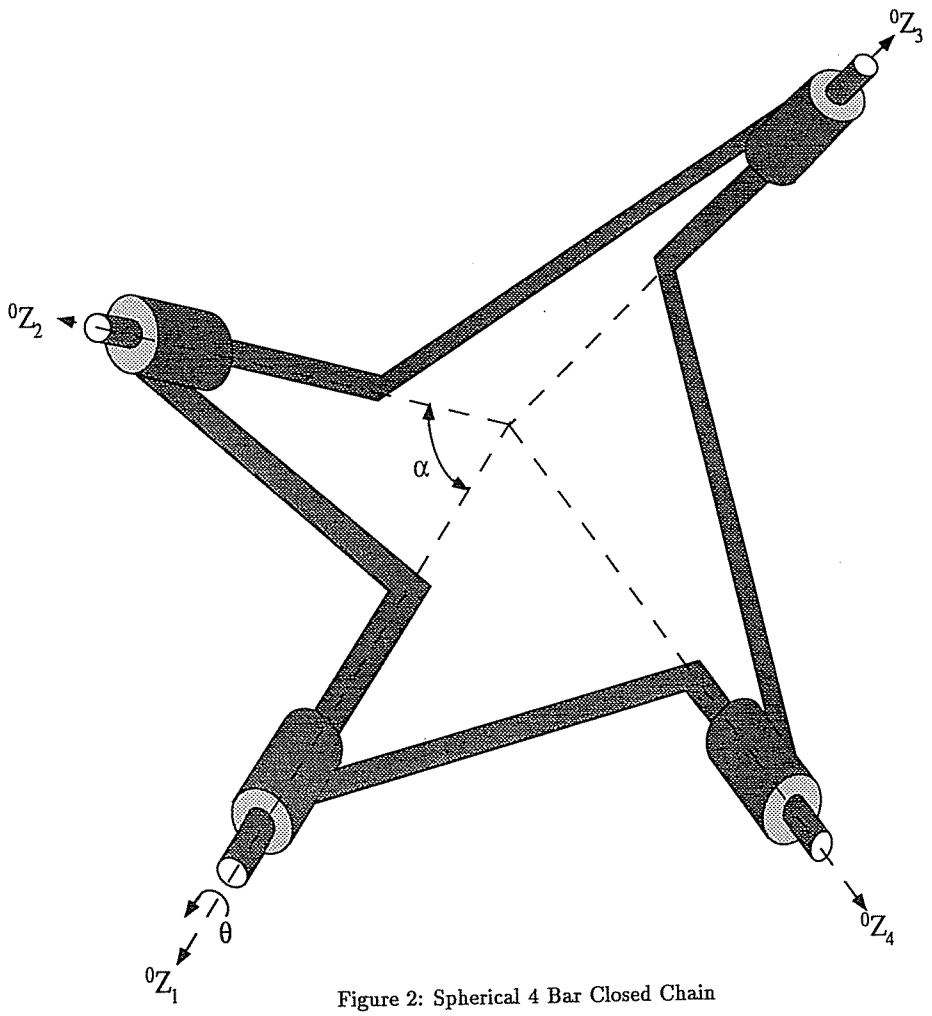

Figure 2: Spherical 4 Bar Closed Chain

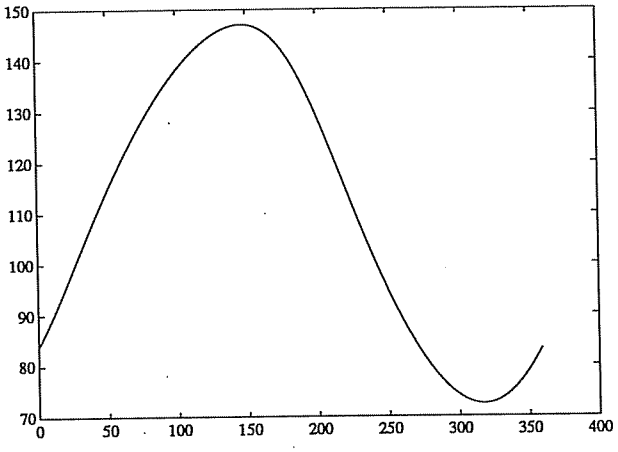

Figure 3: Driven Crank Angle versus Driving Crank Angle

In this example friction is included on the coupler's two moving joints. The coefficient of friction used is $\mu = 0.25$. The criteria used to determine convergence is that the norm of the change in solution was required to be less than 0.10. The driven torque is plotted in Fig. 4. Note that the driven torque has decreased for all driving crank angles. This can be interpreted as the driving torque losing some of its ability to do useful work by having to oppose the friction torques. The internal moments applied to the coupler are plotted in Fig. 6. Note in the presense of friction that the maximum and minimum values of m_{3x} have decreased to 2.3 and 12.2 times the driving torque to the system; respectively. However, the presence of coupler joint friction has induced an internal reaction moment on the coupler about its y axis. This torsional moment, m_{3y}, ranges from 0.6 to 3.3 times the driving torque to the system.

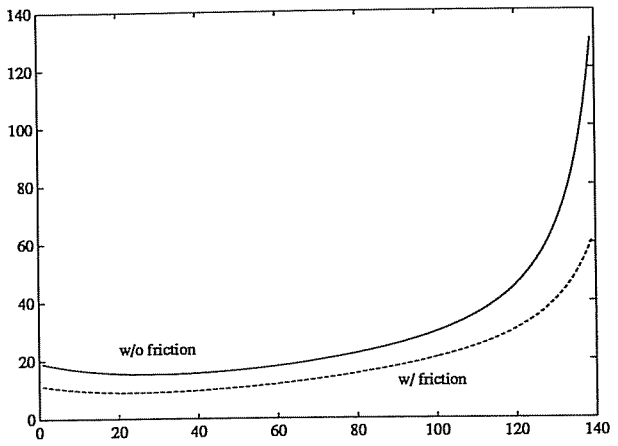

Figure 4: Driven Torque versus Driving Crank Angle

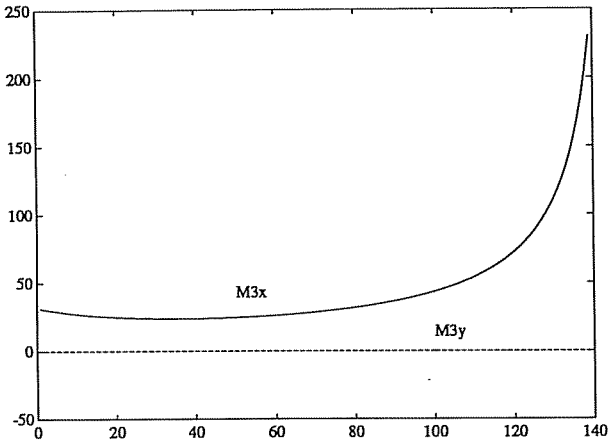

Figure 5: m_{3x} and m_{3y} versus Driving Crank Angle

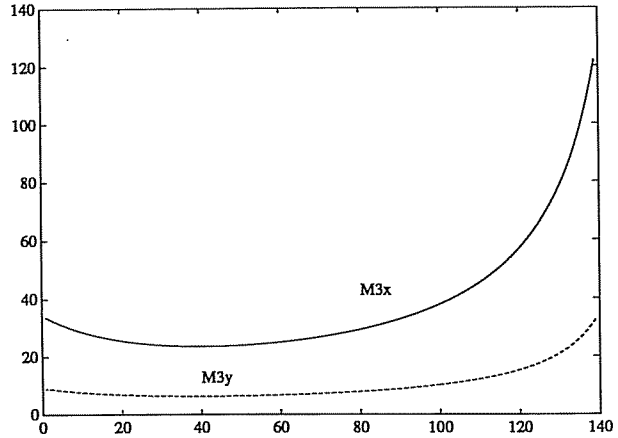

Figure 6: m_{3x} and m_{3y} versus Driving Crank Angle

7 Conclusions

In this article we have presented an algorithm for performing a complete static loading analysis for spherical nR kinematic chains with joint friction. In particular we have examined the case of spherical 4 bar closed chains. In our study of these mechanisms we have found that when approaching singular configurations the bending moments on the coupler become large as the output torque increases. In other configurations the bending moment has a minimum of 2.3 times the driving torque. In addition, we have found joint friction to cause torsional moments on the coupler not present when friction is neglected in the model. It is our expectation that understanding the internal loading will lead to practical spherical mechanisms.

8 Acknowledgements

The support of the National Science Foundation, grant MSM-8720580, is gratefully acknowledged. Furthermore, the aid of Peter Dietmaier was invaluable in creating Fig. 2.

References

[1] Bagci, C., Static Force and Torque Analysis Using 3 × 3 Screw Matrix, and Transmission Criteria for Space Mechanisms *ASME J. Eng. for Ind.* Feb., 1971

[2] Chiang, C.H., *Kinematics of Spherical Mechanisms* Cambridge Press, 1988.

[3] Denavit, J., and Hartenberg, R., A Kinematic Notation for Lower Pair Mechanisms Based on Matrices *ASME J. Appl. Mech.* Vol. 22, 1955.

[4] Duffy, J., *Analysis of Mechanisms and Robotic Manipulators* Wiley and Sons, New York, 1980.

[5] Keler, M.L., Kinematics and Statics Including Friction in Single-Loop Mechanisms by Screw Calculus and Dual Vectors *ASME J. Eng. for Ind.* May, 1973

[6] McCarthy, J.M., *An Introduction to Theoretical Kinematics* MIT Press, 1990.

[7] Yoshikawa, T., *Foundations of Robotics: Analysis and Control* MIT Press, 1990.